Available online at www.sciencedirect.com
ScienceDirect
Catalysis Today 137 (2008) 483–488
CATALYSIS TODAY
www.elsevier.com/locate/cattod

Gold/iron carbonyl clusters as precursors for TiO_2 supported catalysts

Stefania Albonetti [a,*], Rosa Bonelli [a], Joseph Epoupa Mengou [a,c], Cristina Femoni [b], Cristina Tiozzo [b], Stefano Zacchini [b], Ferruccio Trifirò [a]

[a] *Dip. di Chimica Industriale e dei Materiali, Università di Bologna, Viale Risorgimento 4, 40136 Bologna, Italy*
[b] *Dip. Chimica Fisica ed Inorganica, Università di Bologna, Italy*
[c] *Interuniversity Consortium "Chemistry for the Environment" (INCA), Dorsoduro 2137, 30123 Venezia, Italy*

Available online 21 December 2007

Abstract

A series of supported gold/iron catalysts has been prepared from bimetallic carbonyl clusters and characterized to determine how the nature of the precursors and the thermal treatment conditions affected the dispersion of the active phase and the catalytic activity. The chemical–physical characterization, and the catalytic tests carried out, evidenced that the deposition of bimetallic Au/Fe carbonyl clusters on a titania support, and their following controlled decomposition, is a way to obtain stable catalysts, active in the decomposition of toluene.

Keywords: Catalytic combustion; Gold/iron catalysts; Cluster-derivated catalysts

1. Introduction

The use of catalytic systems for pollution abatement has grown tremendously in recent decades due to increasingly restrictive environmental regulations for mobile and stationary sources. In the case of stationary sources one of the most important applications consists in VOCs abatement for which two kinds of catalysts are usually applied: (i) supported noble metals and (ii) metal oxides [1,2]. Various reports have shown that supported Pt and Pd are very efficient catalysts for volatile organic compounds total oxidation [3,4], however cheaper catalytic materials are of ever increasing importance. For instance, it has been recently reported that gold/iron catalysts revealed a high activity in the catalytic oxidation of different alcohols, acetone and toluene [5,6] while Siffert and co-workers [7] reported the promotional effect of gold on palladium for the reaction of catalytic combustion of propene and toluene. In spite of the actual lower activity of these materials with respect to Pt and Pd metals, their relatively low cost has encouraged considerable effort in the tuning of multi-component catalysts suitable for combustion reactions; it is, in fact, well known that the combination of two or more active phases can lead to synergic effects such as increased activity and enhanced catalysts lifetime [8–10]. The catalytic behavior of multi-component supported catalysts is, however, strongly affected by the size of the metal particles and by their reciprocal interactions [11,12] and these properties can be strongly influenced by the method of synthesis.

For the preparation of highly dispersed gold catalysts, specific methods have been used, such us co-precipitation and deposition–precipitation [13–16]. In particular, deposition–precipitation is considered to give the most active catalysts. However, little has been reported so far in the literature regarding supported bimetallic catalysts containing gold [17]. Moreover, conventional techniques, commonly used for the preparation of supported bimetallic particles, involving co-precipitation or co-impregnation, followed by a high-temperature reduction, could strongly affect Au properties, leading to structurally non-uniform materials and high dimension supported particles.

Ligand stabilized metal clusters, with nanometric dimensions, are possible precursors for the preparation of catalytically active nanoparticles with controlled dimensions and compositions [18,19]. Among these, metal carbonyl clusters are quite attractive, since the fact that they can be prepared with several different sizes and composition and, moreover, they are decomposed under very mild conditions [20–23].

Following these considerations, in this paper, we report the results of our first attempts to synthesize gold/iron supported

* Corresponding author. Tel.: +39 051 2093681; fax: +39 051 2093680.
E-mail address: stalbone@fci.unibo.it (S. Albonetti).

0920-5861/$ – see front matter
doi:10.1016/j.cattod.2007.11.003

catalysts utilizing bimetallic carbonyl cluster salts and to elucidate the influence of the preparation conditions on catalyst properties. The complete oxidation of toluene and *o*-dichlorobenzene [24] were used as probe reactions.

2. Experimental

2.1. Catalyst preparation

The catalysts, with different content of Au and Fe, have been prepared by impregnation of the bimetallic carbonyl cluster salts $[NEt_4]_4[Au_4Fe_4(CO)_{16}]$ [25] and $[NEt_4][AuFe_4(CO)_{16}]$ [26] on TiO_2 powder (Millennium Chemicals DT51). In a typical experiment, the required amount of the carbonyl cluster was dissolved in degassed acetone (10–40 mL) under nitrogen and added dropwise over a period of 1 h to an acetone suspension of TiO_2 (10–15 g), previously degassed and stored under nitrogen. The resulting suspension was allowed to stir overnight and, then, the solvent was removed *in vacuum* at room temperature. Finally, the prepared samples were stored in air at ambient temperature and thermally treated at 673 K in flowing N_2. During this last treatment, the temperature was ramped at a rate of $10^\circ\ min^{-1}$ from room temperature to 673 K in order to fully decompose the carbonyl clusters and the ammonium cations. The impregnation process was checked by FTIR in the ν(CO) region at different stages: starting cluster solution; acetone solution in contact with TiO_2; nujol mull of the dried powders before and after thermal treatment. To study the influence of the thermal treatments, sample $Fe_{0.6}Au_2$–Ti was treated in air, N_2 and in H_2 while, to verify the effect of different content of active phase, increasing amounts of $[NEt_4]_4[Au_4Fe_4(CO)_{16}]$ cluster were impregnated on the TiO_2 support. Prepared catalysts are reported in Table 1.

2.2. Characterization of catalysts

Surface areas were measured by N_2 physisorption apparatus (Sorpty 1750 CE Instruments) and single point BET analysis methods, samples were pre-treated under vacuum at 473 K.

XRD measurements were carried out at room temperature with a Bragg/Brentano diffractometer (X'pertPro Panalytical) equipped with a fast X'Celerator detector, using Cu anode as X-ray source (Kα, λ = 1.5418 Å). Data were collected in the 2θ range 10–85°, counting 20 s each 0.05° step.

The coherent length of the Au crystalline domains was evaluated through single line profile fitting of the reflection at 2θ 44.3°, since at this angle no overlap with the anatase pattern of the support is observed. Crystal size values were calculated from the widths at half maximum intensity using the Scherrer equation. IR spectra were recorded with a PerkinElmer SpectrumOne interferometer in CaF_2 cells.

Catalytic experiments were carried out in a fixed bed glass reactor at atmospheric pressure [24]. A K-type thermocouple was placed into the catalyst bed to monitor the reaction temperature. Each run used approximately 350 mg of catalyst in the form of 30–60 mesh (250–595 μm) particles, mixed with 1120 mg of corundum grains of similar size for better temperature control. The total volumetric flow through the catalyst bed was held constant at 140 mL/min, 10 vol.% oxygen, 90 vol.% nitrogen and 1400 ppm of *o*-dichlorobenzene or toluene. Analysis of reactants and products were carried out as follows: the products in the outlet stream were scrubbed in cold acetone maintained at 248 K by a mixture of dry ice and glycol. In the case of *o*-DCB the amounts of reagent and products condensed during a reaction period of 15 min at steady state conditions were analyzed with a GC (PelkinElmer Autosystem XL) equipped with a PE-17 capillary column (30 m × 0.25 mm, methylpolysiloxane series) and an electron capture detector (ECD) which uses 1,2 dichloropropane as a standard reference. Additionally, the exit-flow of the reactor trapped in acetone was injected into a GC with a mass selective detector (Hewlett Packard G1800A) to confirm GC data and to verify the formation of non-chlorinated compounds. Analysis of reactants and products during toluene oxidation were carried out with a GC (HRCG MEGA 2 Series FISONS Instruments) equipped with a HP-5 capillary column and a FID. For both reaction CO and CO_2 formed were separated on a capillary column Elite Plot Q (30 m × 0.32 mm), attached to a methanizer and analyzed with a flame ionization detector (FID). Particular care was devoted to determination of the C

Table 1
Code name, composition and thermal treatment conditions of studied catalysts

Catalyst	Fe/Au precursor	Pretreatment conditions	Fe content (wt. %)	Au content (wt. %)
TiO_2	-	Air at 673 K	0	0
$Fe_{0.6}Au_{0.6}$-Ti-O_2	$[NEt_4][AuFe_4(CO)_{16}]$	Air at 673 K	0.6	0.6
$Fe_{0.6}Au_2$-Ti	$[NEt_4]_4[Au_4Fe_4(CO)_{16}]$	Not calcined	0.6	2.0
$Fe_{0.6}Au_2$-Ti-O_2	$[NEt_4]_4[Au_4Fe_4(CO)_{16}]$	Air at 673 K	0.6	2.0
$Fe_{0.6}Au_2$-Ti-N_2	$[NEt_4]_4[Au_4Fe_4(CO)_{16}]$	N_2 at 673 K	0.6	2.0
$Fe_{0.6}Au_2$-Ti-H_2	$[NEt_4]_4[Au_4Fe_4(CO)_{16}]$	H_2 at 673 K	0.6	2.0
$Fe_{1.2}Au_4$-Ti	$[NEt_4]_4[Au_4Fe_4(CO)_{16}]$	Not calcined	1.2	4.0
$Fe_{1.2}Au_4$-Ti-N_2	$[NEt_4]_4[Au_4Fe_4(CO)_{16}]$	N_2 at 673 K	1.2	4.0
$Fe_{1.8}Au_6$-Ti	$[NEt_4]_4[Au_4Fe_4(CO)_{16}]$	Not calcined	1.8	6.0
$Fe_{1.8}Au_6$-Ti-N_2	$[NEt_4]_4[Au_4Fe_4(CO)_{16}]$	N_2 at 673 K	1.8	6.0

balance, which was found to always fall between 95 and 105% (calculated as the comparison between converted *o*-dichlorobenzene and the sum of the product yields).

3. Results and discussion

3.1. Preparation and characterization of the supported catalysts

Two different Au–Fe carbonyl clusters have been employed along this work for the preparation of the supported catalysts, i.e. $[NEt_4]_4[Au_4Fe_4(CO)_{16}]$ [25] and $[NEt_4][AuFe_4(CO)_{16}]$ [26]. These two bimetallic clusters not only have a different Au:Fe composition but, quite interestingly, have a different chemical behaviour. Thus, whereas $[NEt_4][AuFe_4(CO)_{16}]$ is quite stable and non-reactive, $[NEt_4]_4[Au_4Fe_4(CO)_{16}]$ is very reactive, being easily oxidised yielding other Au–Fe carbonyl species. Moreover, the final product of its oxidation is $[NEt_4][AuFe_4(CO)_{16}]$, making the two species close in relationship. Several other Au–Fe carbonyl clusters exist in between these two species, even though none of them has been, up to now, completely characterised. Nonetheless, some information on their nature can be obtained from the analogous Ag–Fe carbonyl clusters system, from which is known that oxidation of the $[Ag_4Fe_4(CO)_{16}]^{4-}$ anion results, first, in the formation of $[Ag_5Fe_4(CO)_{16}]^{3-}$ and, then, $[Ag_{13}Fe_8(CO)_{32}]^{n-}$ (n = 3–5) [27,28]. The analogy between the Au–Fe and Ag–Fe systems is supported by the similarities of the IR spectra of the intermediates for the oxidation of $[Au_4Fe_4(CO)_{16}]^{4-}$ and $[Ag_4Fe_4(CO)_{16}]^{4-}$.

This chemical behaviour displayed in solution is very well paralleled by the present work on the interaction of $[NEt_4]_4[Au_4Fe_4(CO)_{16}]$ [ν(CO) 1931(s) and 1861(s) cm^{-1}] and $[NEt_4][AuFe_4(CO)_{16}]$ [ν(CO) 2018(s) cm^{-1}] with TiO_2.

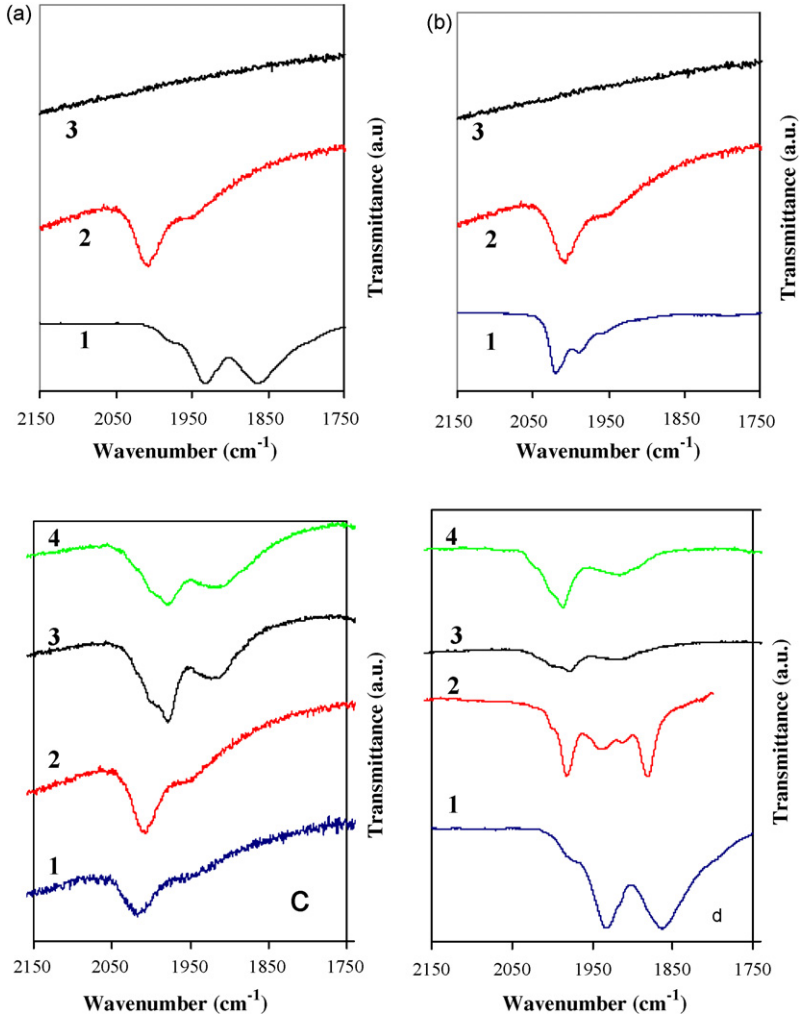

Fig. 1. (a) FTIR spectra in the ν(CO) region obtained during the preparation of the Au–Fe catalyst on TiO_2 (2 wt.% Au) from $[NEt_4]_4[Au_4Fe_4(CO)_{16}]$: (1) $[NEt_4]_4[Au_4Fe_4(CO)_{16}]$ in acetone; (2) nujol mull spectrum of the impregnated powder after removal *in vacuum* of the solvent; (3) nujol mull spectrum after thermal treatment in air. (b) FTIR spectra in the ν(CO) region obtained during the preparation of the Au–Fe catalyst on TiO_2 from $[NEt_4][AuFe_4(CO)_{16}]$: (1) $[NEt_4][AuFe_4(CO)_{16}]$ in acetone; (2) nujol mull spectrum of the impregnated powder after removal *in vacuum* of the solvent; (3) nujol mull spectrum after thermal treatment in air. (c) FTIR spectra in nujol mull in the ν(CO) region of the powders dried *in vacuum* after impregnation on TiO_2 of $[NEt_4]_4[Au_4Fe_4(CO)_{16}]$: (1) 1 wt.% Au; (2) 2 wt.% Au; (3) 4 wt.% Au; (4) 6 wt.% Au. (d) FTIR spectra in the ν(CO) region obtained during the impregnation on TiO_2 of $[NEt_4]_4[Au_4Fe_4(CO)_{16}]$ (4 wt.% Au): (1) $[NEt_4]_4[Au_4Fe_4(CO)_{16}]$ in acetone; (2) the acetone solution after being in contact with TiO_2; (3) the powder (in nujol mull) after removal *in vacuum* of the solvent; (4) the CH_3CN extraction from the dried powder.

Hence, no reaction has been observed by adding an acetone solution of $[NEt_4][AuFe_4(CO)_{16}]$ to TiO_2, nor after removal of the solvent *in vacuum* (Fig. 1b). Conversely, $[NEt_4]_4[Au_4Fe_4(CO)_{16}]$ is oxidised under the same conditions (Fig. 1a) as indicated by the increased ν(CO) wave numbers, following the behaviour observed in solution. The product obtained depends on the cluster: TiO_2 ratio (Fig. 1c); in following this process it is noteworthy to remember that for carbonyl species, in general, the more oxidised species display higher ν(CO), due to a decreased π-back donation from the metal to CO. Therefore, it is cleat from Fig. 1c, that the degree of oxidation of the clusters increases by decreasing the cluster: TiO_2 ratio. Moreover, the oxidation process occurs in two different moments during catalyst preparation, as can be inferred from Fig. 1d, where we have reported the FTIR spectra in the ν(CO) region of: (1) $[NEt_4]_4[Au_4Fe_4(CO)_{16}]$ in acetone [ν(CO) 1931(s) and 1861(s) cm^{-1}]; (2) the acetone solution after being in contact with TiO_2 [ν(CO) 1982(s), 1940(m), 1913(w) and 1881(s) cm^{-1}]; (3) the powder (in nujol mull) after removal *in vacuum* of the solvent [ν(CO) 2000(sh), 1978(s) and 1917(m) cm^{-1}]; (4) the CH_3CN extraction from the (3) dried powder [ν(CO) 2000(sh), 1986(s) and 1914(m) cm^{-1}]. From this is clear that as soon as the acetone solution of $[Au_4Fe_4(CO)_{16}]^{4-}$ gets in contact with TiO_2 the cluster reacts giving more oxidised species, of the type $[Au_5Fe_4(CO)_{16}]^{3-}$ [ν(CO) 1944(s) and 1831(s) cm^{-1}] and $[Au_{13}Fe_8(CO)_{32}]^{n-}$ [ν(CO) 1986(s) and 1931(m) cm^{-1}], depending on the cluster: TiO_2 ratio; the more cluster is added, the less oxidation is observed. The latter species contain an Au:Fe ratio higher than the precursor $[Au_4Fe_4(CO)_{16}]^{4-}$; the excess iron is released in the form of $[HFe(CO)_4]^-$ as indicated by the ν(CO) at 1881 cm^{-1} in FTIR spectra of the acetone solution (Fig. 1d (2)). The oxidant is likely to be TiO_2 and, therefore, Ti(IV) is partially reduced, as indicated by the fact that the solid turns from white to grey. This is also in agreement with the fact that the degree of oxidation of the cluster increases by increasing the amount of TiO_2 (lower wt% Au). Further reaction, then, occurs when the carbonyl species are forced to get in closer contact with TiO_2 by removal *in vacuum* of the solvent, as indicated by the change in the FTIR spectrum (Fig. 1d (3)). The carbonyl species present at this point on the solid support can be, then, extracted with a polar solvent such as CH_3CN and this makes easier to compare their IR features with the ones reported for the Au–Fe carbonyl clusters studied in solution (Fig. 1d (4)). This analysis confirms that the species present on the solid supports at the end of the deposition process are oxidised clusters such as $[Au_{13}Fe_8(CO)_{32}]^{n-}$ and $[AuFe_4(CO)_{16}]^-$; the former species is favoured by a high load of cluster (4–6 wt.% Au), whereas the latter increases by lowering the amount of cluster (1–2 wt.% Au). Oxidation of $[HFe(CO)_4]^-$ is observed, too, yielding mainly $[HFe_3(CO)_{11}]^-$ [ν(CO) 2000(s) cm^{-1}] as also confirmed by independent experiments where $[HFe(CO)_4]^-$ has been directly deposited on TiO_2 following the same procedure.

After storing the dried powder in air for one night, all the supported carbonyl clusters are decomposed, as confirmed by the complete disappearance of any ν(CO) from the FTIR spectra. Moreover, the powders assume the typical purple colour of highly dispersed gold metal. Finally, complete decomposition of the organic cations has been achieved by thermal treatment, either on air or under controlled atmosphere. The characteristics of these catalytic materials and the effects on them of the carbonyl precursor employed, its amount and the thermal treatment conditions are, then, described below.

Table 2 lists BET surface areas of the prepared catalysts and evidences that this parameter remains unchanged after gold/iron deposition, thus indicating that Au and FeO_x particles did not block the pore of the support.

Table 2
BET specific surface area and Au average crystallite size for studied catalysts

Catalyst	Surface area (m^2/g)	Au particle size Fresh (nm)	Au particle size DCB[a] used (nm)	Au particle size TOL[b] used (nm)
TiO_2	80	-	-	-
$Fe_{0.6}Au_{0.6}$-Ti-O_2	61	-	-	-
$Fe_{0.6}Au_2$-Ti	-	3.4	-	-
$Fe_{0.6}Au_2$-Ti-O_2	81	23.1	38.8	-
$Fe_{0.6}Au_2$-Ti-N_2	80	6.0	24.9	6.0
$Fe_{0.6}Au_2$-Ti-H_2	76	5.2	20.1	-
$Fe_{1.2}Au_4$-Ti	-	5.9	-	-
$Fe_{1.2}Au_4$-Ti-N_2	79	6.6	28.7	6.7
$Fe_{1.8}Au_6$-Ti	-	7.0	-	-
$Fe_{1.8}Au_6$-Ti-N_2	71	7.4	-	7.6

Au averaged particle size were calculated from XRD diffrattograms using the Sherrer formula. [a]Catalysts tested in the total oxidation of *o*-dichlorobenzene. [b]Catalysts tested in the total oxidation of toluene.

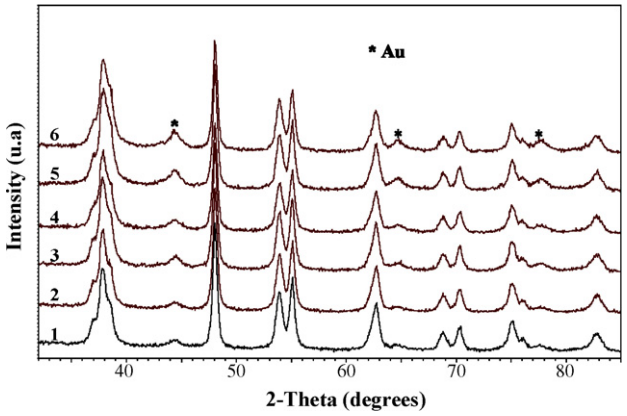

Fig. 2. XRD patterns of catalysts fresh and used in the complete oxidation of toluene with increasing content of active phase: $Fe_{0.6}Au_2$–Ti–N_2 (1, fresh; 2, used), $Fe_{1.2}Au_4$–Ti–N_2 (3, fresh; 4, used), $Fe_{1.8}Au_6$–Ti–N_2 (5, fresh; 6, used).

Fig. 2 reports the XRD patterns for the gold/iron catalysts thermally treated under nitrogen with increasing content of gold. The graph reports the comparison between fresh samples and materials used in the reaction of toluene oxidation. For all synthesized samples excluding $Fe_{0.6}Au_{0.6}$–Ti–O_2, the XRD patterns present, besides the characteristic peaks of the TiO_2 support (anatase phase), weak reflections due to the presence of gold. No diffraction peaks of metallic iron or FeO_x compounds were observed. The intensities of gold peaks slightly increased with the gold loading. The average Au particles sizes for all prepared samples, as determined from XRD line broadening, are given in Table 2. The mean gold particle sizes of samples before thermal treatment increased from 3 to 7 nm as the Au loading increased from 2 to 6 wt.%. Moreover, the Au crystallites were found to significantly sinter during the calcination in air but did not greatly change after thermal treatment under N_2 and H_2, especially for samples with higher amount of Au. These data indicate an appreciable agglomeration of gold particles upon calcination in air but underline the possibility to direct the size of gold particles by controlling cluster oxidation/decomposition. Moreover, the characterization of the used catalysts evidenced a significant Au particles sintering during *o*-DCB combustion but a substantial stability during toluene total oxidation.

3.2. Activity measurements

On this paper, we report a preliminary study on the total oxidation of two representative organic compounds, i.e. *o*-dichlorobenzene and toluene, often utilized as probe molecules for chlorinated organics and VOC. Fig. 3a shows the conversion of *o*-dichlorobenzene as a function of the reaction temperature. Although previous papers reported high activity and stability of Au containing catalysts in the total oxidation of chlorinated compounds [29,30], our Au/Fe supported catalysts resulted not

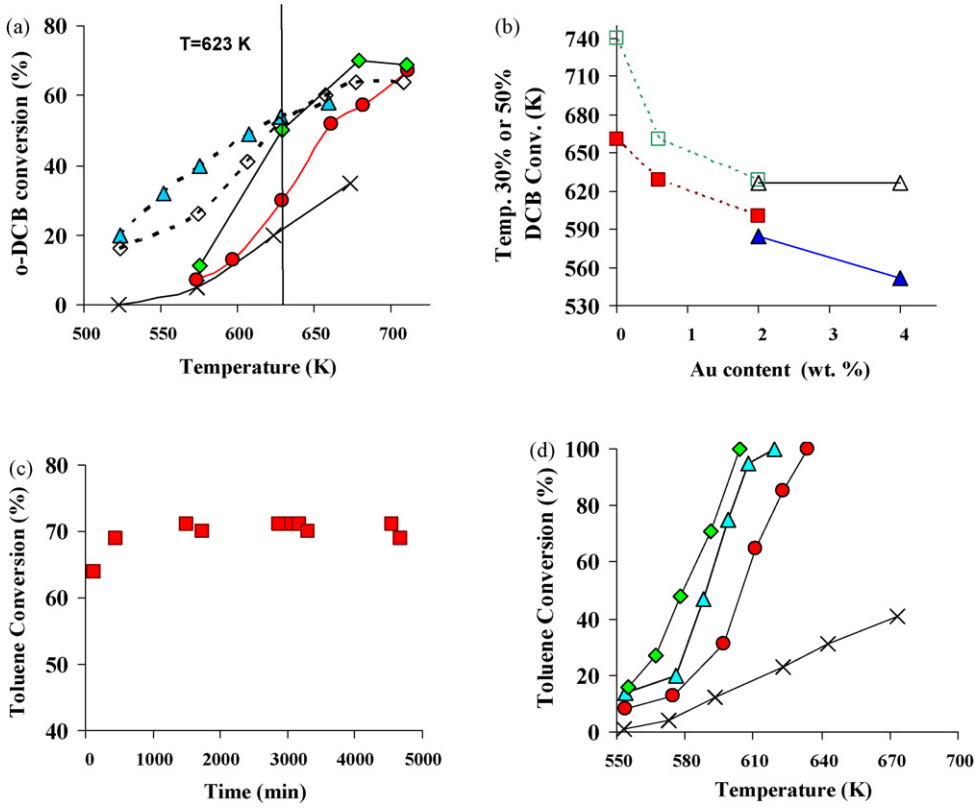

Fig. 3. (a) *o*-DCB conversion as a function of reaction temperature for air (solid line) and nitrogen (dotted line) thermal treated Au/FeO_x/TiO_2 samples. TiO_2 (×), $Fe_{0.6}Au_{0.6}$–Ti–O_2 (●), $Fe_{0.6}Au_2$–Ti–O_2 (◆), $Fe_{0.6}Au_2$–Ti–N_2 (◇), $Fe_{1.2}Au_4$–Ti–N_2 (△). (b) Temperature of 30% (filled symbols) and 50% (open symbols) conversion of 1400 ppm *o*-DCB as a function of the Au content for the Au/FeO_x/TiO_2 samples calcined in N_2 (▲, △) and air (■, □). (c) Long-term activity test on $Fe_{1.8}Au_6$–Ti–N_2 sample. Toluene conversion at 591 K as a function of time. (d) Toluene conversion as a function of reaction temperature for Fe/Au catalysts at different content of active phase. TiO_2 (×), $Fe_{0.6}Au_2$–Ti–N_2 (●), $Fe_{1.2}Au_4$–Ti–N_2 (△), $Fe_{1.8}Au_6$–Ti–N_2 (◆).

stable in chlorinated containing stream, especially at high reaction temperatures (623–673 K). Moreover, despite the fact that the main oxidation products formed during *o*-DCB destruction were CO and CO_2, significant amount of other chlorinated by-products were detected. Nevertheless, these data enable interesting observations that can be better explained observing the Fig. 3b, reporting the temperature necessary to have 30 and 50% *o*-DCB conversion, as a function of Au content in the different materials. Thus, at reaction temperature lower than 623 K, the *o*-DCB conversion significantly depends on Au content and Au particle size; in fact, the temperature necessary to have 30% *o*-DCB conversion considerably decreases with increasing the Au amount on the catalysts. Moreover, the $Fe_{0.6}Au_2$–Ti sample calcined in N_2 ($Fe_{0.6}Au_2$–Ti–N_2), having Au crystallites of about 6 nm, are more active than sample calcined in air ($Fe_{0.6}Au_2$–Ti–O_2) that present higher Au particle dimension (23 nm). Notwithstanding, at higher temperatures, the deactivation effect is more evident. In fact, the catalytic activity of samples calcined under nitrogen falls more rapidly than that of materials thermally treated in air leading to materials with no significant difference in the temperature necessary to have 50% *o*-DCB conversion. Moreover, the analysis by XRD of materials after catalytic reaction provides evidence for significant sintering of the Au particle during the *o*-DCB total oxidation (Table 2).

On the contrary, all the iron/gold cluster-derived catalysts showed an excellent stability under catalytic condition in toluene total oxidation, as reported in Fig. 3c. In fact, after slight activation, during the first 2 h of run, the Au/FeO_x–TiO_2 remained perfectly stable for the further 80 h. Moreover, Fig. 3d, reporting the conversion of toluene as a function of reaction temperature, indicated that increasing the amount of Au/Fe cluster over titania enhances the combustion activity. In particular, in the sample with the highest amount of metals ($Fe_{1.8}Au_6$–Ti–N_2), the reaction temperature necessary to have 50% of toluene conversion was 578 K compared with 603 K in $Fe_{0.6}Au_2$–Ti–N_2. In addition, it must be underlined that, on the toluene oxidation, no formation of partial oxidation products was revealed and CO_2 is the only product formed.

4. Conclusions

This paper describes the synthesis, characterization and catalytic behavior of Au/FeO_x/TiO_2 catalysts synthesized using gold/iron carbonyl clusters as the precursors. The novel preparation method resulted in small gold nanoparticles already after air exposure at ambient temperature and, depending on the gas atmosphere utilized during thermal treatments; highly dispersed metallic gold can be formed at 673 K. The prepared materials are active for toluene oxidation and the catalytic activity depends on the Fe/Au cluster loading over TiO_2. Structural characterization of these catalysts by TEM and other techniques and a detailed investigation on the parameters affecting the catalytic activity of several Au/FeO_x/TiO_2 catalysts is currently in progress.

Acknowledgement

We thank the University of Bologna (Project CLUSTER-CAT) for funding.

References

[1] S.C. Kim, J. Hazard. Mater. B91 (2002) 285.
[2] P. Gélin, M. Primet, Appl. Catal. B 39 (2002) 1.
[3] G. Centi, J. Mol. Catal. A 173 (2001) 287.
[4] K. Okumura, T. Kobayashi, H. Tanaka, M. Niwa, Appl. Catal. B 44 (2003) 325.
[5] S. Minicò, S. Scirè, C. Crisafulli, R. Maggiore, S. Galvagno, Appl. Catal. B 28 (2000) 245.
[6] S. Minicò, S. Scirè, C. Crisafulli, S. Galvagno, Appl. Catal. B 34 (2001) 277.
[7] M. Hosseini, S. Siffert, H.L. Tidahy, R. Cousin, J.-F. Lamonier, A. Aboukais, A. Vantomme, M. Roussel, B.-L. Su, Catal. Today 122 (2007) 391.
[8] L. Guczi, Catal. Today 101 (2005) 53.
[9] T. Miyake, T. Asakawa, Appl. Catal. A 280 (2005) 47.
[10] N. Toshima, T. Yonezawa, New J. Chem. 22 (1998) 1179.
[11] M. Haruta, Catal. Today 36 (1997) 153.
[12] M.A.P. Dekkers, M.J. Lippits, B.E. Nieuwenhuys, Catal. Today 54 (1999) 381.
[13] M. Haruta, M. Datè, Appl. Catal. A 6 (2002) 102.
[14] T.V. Choudhary, D.W. Goodman, Top. Catal. 21 (2002) 25.
[15] H.H. Kung, M.C. Kung, C.K. Costello, J. Catal. 216 (2003) 425.
[16] A.S.K. Hashmi, G.J. Hutchings, Angew. Chem. Int. Ed. 45 (2006) 789.
[17] L.B. Ortiz-Soto, O.S. Alexeev, M.D. Amiridis, Langmuir 22 (2006) 3112.
[18] J.A. Scwarz, C. Contescu, Chem. Rev. 95 (1995) 477.
[19] Yu.I. Yermakov, B.N. Kuznetsov, J. Mol. Catal. 9 (1980) 13.
[20] M. Ichikawa, in: P. Braunstein, L.A. Oro, P.R. Raithby (Eds.), Metal Clusters in Chemistry, Wiley-VCH, 1999, p. 1273.
[21] B.C. Gates, Chem. Rev. 95 (1995) 511.
[22] J.M. Thomas, B.F.G. Johnson, R. Raja, G. Sankar, P.A. Midgley, Acc. Chem. Res. 36 (2003) 20.
[23] R. Psaro, S. Recchia, Catal. Today 41 (1998) 139.
[24] S. Albonetti, S. Blasioli, A. Bruno, J. Epoupa Mengou, F. Trifirò, Appl. Catal. B 64 (2006) 1.
[25] V.G. Albano, F. Calderoni, M.C. Iapalucci, G. Longoni, M. Monari, Chem. Commun. (1995) 433.
[26] V.G. Albano, R. Aureli, M.C. Iapalucci, F. Laschi, G. Longoni, M. Monari, P. Zanello, Chem. Commun. (1993) 1501.
[27] V.G. Albano, F. Azzaroni, M.C. Iapalucci, G. Longoni, M. Monari, S. Mulley, D.M. Proserpio, A. Sironi, Inorg. Chem. 33 (1994) 5320.
[28] V.G. Albano, F. Calderoni, M.C. Iapalucci, G. Longoni, M. Monari, P. Zanello, J. Cluster Sci. 6 (1995) 107.
[29] B. Chen, C. Bai, R. Cook, J. Wright, C. Wang, Catal. Today 30 (1996) 15.
[30] T. Aida, R. Higuchi, H. Niiyama, Chem. Lett. (1990) 2247.